On the accuracy of a regional geoid

Mehdi Najafi[1*]), Petr Vaníček[1], Peng Ong[2],
and Michael R. Craymer[3]

[1]Department of Geodesy and Geomatics Engineering,
University of New Brunswick,
Fredericton, N.B. E3B 5A3, Canada

[2]Apt. Blk. 203 Petir Road
08-655 Singapore 670203

[3]Geodetic Survey Division,
Geomatics Canada, 615 Booth Street,
Ottawa, Ontario K1A 0E9, Canada

Abstract

In the Stokes-Helmert method deployed at UNB, the geoid is determined in two steps, with different type of data used in each step. The first step consists of selecting a higher-degree reference spheroid using a satellite-derived potential field (potential coefficients), estimated from satellite tracking observations. In the second step, the residual geoid is determined from terrestrial gravity anomalies. Uncertainties of the potential coefficients are propagated to the spheroid according to the law of propagation of (random error) covariance matrices. In the residual geoid, errors in the gravity data are propagated through the (modified spheroidal) Stokes integral to yield point variances. Neglecting the correlations among individual gravity anomalies, the correlation between any two residual geoidal heights is a function of the area covered by gravity anomalies used in common by the Stokes integrals at the two points.

*) First author's present address: University of K. N. Toosi, Faculty of Civil Engineering, Dept. of Surveying Engineering, Mirdamad intersection, No. 1346 Valiasr st., Tehran, Iran.

1 Introduction

The accuracy of both a geoidal height at a point, as well as the geoidal height difference between two neighbouring points is investigated here. This accuracy depends on the observational uncertainties of the data used, as well as on the method used for the geoid determination.

In the Stokes-Helmert method employed here [Vaníček and Martinec, 1994], the geoid is determined in two parts: the long wavelength part, and the short wavelength part. The long wavelength part, also called the reference spheroid [Vaníček et al., 1986] describes the global variations of the geoid. It is determined from satellite-derived potential coefficients. The remaining part called the residual (high-frequency) geoid describes the local variations of the geoid. It is determined from terrestrial gravity data by the generalized Stokes integral.

The reference spheroid of degree L (N_L) is expressed as a finite series of spherical harmonics. Using spherical approximation [Vaníček and Krakiwsky, 1986], we get

$$N_L(\Omega) \;=\; R \sum_{n=2}^{L} T_n(\Omega) \;, \tag{1}$$

where $T_n(\Omega)$ are the surface harmonics of the disturbing potential, given by

$$T_n(\Omega) \;=\; \sum_{m=0}^{n} \left[\overline{T}^{C}_{nm}\, \overline{Y}^{C}_{nm}(\Omega) \;+\; \overline{T}^{S}_{nm}\, \overline{Y}^{S}_{nm}(\Omega) \right] \;, \tag{2}$$

and

$$\begin{bmatrix} \overline{Y}^{C}_{nm}(\Omega) \\ \overline{Y}^{S}_{nm}(\Omega) \end{bmatrix} \quad = \quad \begin{pmatrix} \cos\; m\lambda \\ \sin\; m\lambda \end{pmatrix} \overline{P}_{nm}(\sin\; \varphi) \tag{3}$$

are the fully normalized spherical harmonics [Heiskanen and Moritz, 1981, Eqns. (1-73)]. In the formulae above, R is the mean radius of the earth, Ω is the geocentric direction defined by geocentric latitude φ and longitude λ, and $\overline{T}^{C}_{nm}$, $\overline{T}^{S}_{nm}$ are the fully normalized satellite-derived unitless disturbing potential coefficients.

The high-frequency geoid is determined from the generalized Stokes integral, using a modified spheroidal Stokes's kernel S^{*L} [Vaníček and Kleusberg, 1987; Vaníček and Sjöberg, 1991]

$$\delta N^{L}(\Omega) \;\doteq\; K \iint_{C_0} \delta\Delta g^{L}(\Omega')\; S^{*L}[\; \psi(\Omega,\Omega')\;]\; d\Omega' \;, \tag{4}$$

where

$$K \;=\; \frac{R}{4\pi\gamma_0} \;, \tag{5}$$

Ω' is the integration variable, ψ is the spherical distance between directions Ω and Ω', γ_0 is the normal gravity on the reference ellipsoid, and C_0 denotes the integration domain: a spherical cap of radius $\psi_0 = 6°$ in our applications, and $\delta\Delta g^L$ is the residual gravity anomaly

$$\delta\Delta g^L \;=\; \Delta g \;-\; \Delta g_L \;, \tag{6}$$

where Δg is the "observed" gravity anomaly and Δg_L is the (low-frequency) reference gravity anomaly. The modification of the kernel is carried out in a way that the integration truncated at 6° distance, leaves minimum error on the geoidal height. This error is called the truncation error, or the far-zone contribution, which is estimated from a high resolution global geopotential model, e.g., the GFZ93A model [Gruber and Anzenhofer, 1993].

The generalized Stokes integral acts as a high-pass filter which automatically cuts off the long wavelength contribution of the terrestrial data and refers the (high-frequency) residual geoid to the spheroid. We note that when the far-zone contribution is added to the result of the generalized Stokes integral, we obtain the exact value of the residual geoidal height. Hence, the geoid at each point is determined as the sum of the spheroid (N_L) and the residual geoid (δN^L),

$$N \;=\; N_L \;+\; \delta N^L \;, \tag{7}$$

where the degree L is the degree of the spheroid, 20 in our application [Vaníček and Krakiwsky, 1986, Sec. (23-4)].

2 Variance of the Spheroid of Degree L

For simplicity, let us omit the subscript L from the relevant symbols in this section, bearing in mind that all the discussion here is related to the spheroid of degree L. Uncertainties in the disturbing potential coefficients are due to errors in the satellite potential coefficients estimated from satellite tracking. To estimate σ_N^2, the variance of the spheroid, let us denote by $(\sigma^c_{nm})^2$, $(\sigma^s_{nm})^2$ the error variance of either cosine ($\overline{T}^C_{nm}$) or sine ($\overline{T}^S_{nm}$) satellite potential coefficients in Eqn. (2). By applying the covariance law to the Eqn. (2), we get

$$\sigma_n^2(\Omega) \;=\; \sum_{m=0}^{n} \left[\; (\sigma^c_{nm})^2 \; \left(\overline{Y}^C_{nm}\right)^2 \;+\; (\sigma^s_{nm})^2 \; \left(\overline{Y}^S_{nm}\right)^2 \; \right] \;, \tag{8}$$

where the sum in the square brackets (amplitude of the spherical harmonics) is derived from Eqn. (3). In practice, σ^c_{nm}, σ^s_{nm} will be almost the same for any n and m. In fact, a case can be made that they should really be the same as dependence on longitude cannot

be expected. Putting $\sigma^c_{nm} = \sigma^s_{nm} = \sigma_{nm}$ results in

$$\sigma^2_n(\Omega) \;=\; \sigma^2_n(\varphi) \;=\; \sum_{m=0}^{n} \overline{P}^2_{nm}(\sin\ \varphi)\ \sigma^2_{nm}\ , \tag{9}$$

where $\sigma^2_n(\varphi)$ is the error variance of the surface harmonic T_n and σ^2_{nm} are the estimated error variances from the orbit analysis. The error variances $\sigma^2_n(\varphi)$ for the GRIM4-S4 "satellite only" model with respect to degree n in different latitudes are shown in Fig. (1).

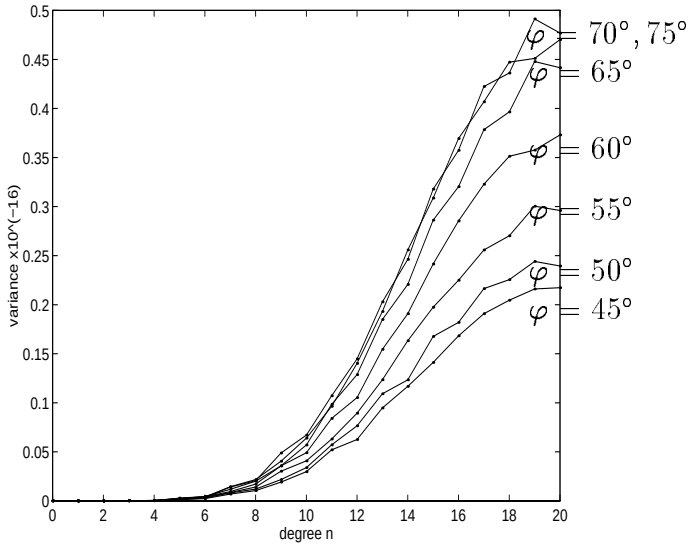

Figure 1: Accuracy performance (error variance in units of 10^{-16}) of the GRIM4-S4 model in different latitudes

Applying now the covariance law to Eqn. (1) yields

$$\sigma^2_N(\varphi) \;=\; R^2 \sum_{n=2}^{L} \sigma^2_n(\varphi)\ , \tag{10}$$

where $\sigma^2_N(\varphi)$ is the error variance of the spheroid, a function of the latitude of the computation point.

Let us look now at ΔN, the spheroidal height difference between points P_i and P_j,

$$\Delta N \;=\; N_j \;-\; N_i\ . \tag{11}$$

The spheroidal heights N_i and N_j, determined from satellite potential coefficients at two points, are statistically correlated. The correlation comes from the fact that the same

potential coefficients are used in both computations. Applying the covariance law to Eqn. (11), the error variance of ΔN is obtained as

$$\sigma^2_{\Delta N} \;=\; \sigma^2_N(\Omega_i) \;+\; \sigma^2_N(\Omega_j) \;-\; 2\; C_N(\Omega_i, \Omega_j)\;, \tag{12}$$

where σ^2_N is given by Eqn. (10) and C_N is the error covariance function. It is expressed in terms of the error correlation function ρ_N as

$$C_N(\Omega_i, \Omega_j) \;=\; \rho_N(\Omega_i, \Omega_j)\; \sigma_N(\Omega_i)\; \sigma_N(\Omega_j)\;. \tag{13}$$

To estimate $\sigma^2_{\Delta N}$, one has to estimate the two variances $\sigma^2_N(\Omega_i)$, $\sigma^2_N(\Omega_j)$, and the value of $C_N(\Omega_i, \Omega_j)$.

To derive the error covariance $C_N(\Omega_i, \Omega_j)$, let us assume a vector of spheroidal heights $\boldsymbol{N}$ computed at a mesh of m points, using satellite-derived coefficients (see Eqns. 1 and 2). Let $\boldsymbol{\Phi}$ be the Vandermonde matrix comprised of the spherical harmonic functions and $\boldsymbol{t}$ the vector of satellite-derived coefficients for the disturbing potential T (Eqn. 2). The following matrix equation is then valid

$$\boldsymbol{N} \;=\; \boldsymbol{\Phi}^T\, \boldsymbol{t}\;. \tag{14}$$

There is an estimated error covariance matrix associated with the vector $\boldsymbol{t}$, derived from the adjustment of the satellite observations. Let us denote it by $\hat{\boldsymbol{C}}_t$. As the spherical harmonic functions are globally orthogonal, the $\hat{\boldsymbol{C}}_t$ matrix is diagonal. Applying the covariance law to Eqn. (14) yields the error covariance matrix of (the vector of spheroidal heights) $\boldsymbol{N}$

$$\boldsymbol{C}_N \;=\; \boldsymbol{\Phi}^T\, \hat{\boldsymbol{C}}_t\, \boldsymbol{\Phi}\;. \tag{15}$$

The error covariance $C_N(\Omega_i, \omega_j)$, the element located at i-th row and j-th column of the matrix $\boldsymbol{C}_N$, is obtained from a quadratic form

$$C_N(\Omega_i, \Omega_j) \;=\; \Phi_i^T\; \hat{\boldsymbol{C}}_t\; \Phi_j\;, \tag{16}$$

where Φ_i and Φ_j are the i-th and j-th columns of the Vandermonde matrix. As the matrix $\hat{\boldsymbol{C}}_t$ is diagonal, and considering Eqns. (1) and (2), we obtain

$$C_N(\Omega_i, \Omega_j) = R^2 \sum_{n=2}^{L} \sum_{m=0}^{n} \sigma^2_{nm} \left[\; \overline{Y}^C_{nm}(\Omega_i)\; \overline{Y}^C_{nm}(\Omega_j) + \overline{Y}^S_{nm}(\Omega_i)\; \overline{Y}^S_{nm}(\Omega_j) \;\right]\;, \tag{17}$$

where σ^2_{nm} is the error variance of the satellite coefficients, Ω_i and Ω_j are the directions of points P_i and P_j.

The covariance function can now be computed, given the accuracy of the satellite coefficients. Fig. 2 illustrates the error variance of N as a function of degree n (σ^2_n =

$\sum_{m=0}^{n} 2\sigma_{nm}^2$), called the error power spectrum of the gravity field determination of the GRIM4-S4 global geopotential model [Schwintzer et al., 1995]. Fig. 3 shows the covariance function of $N(\Omega_i)$ and $N(\Omega_j)$ (Eqn. 17), along a meridian of the spheroid of degree 20, determined by the same model.

We note here that if σ_{nm} in the above formulae were not dependent on m, i.e., if for all m we could write $\sigma_{nm} = \sigma_n$, then Eqn. (17) would reduce to [Sideris and Schwartz, 1987]

$$C_N(\Omega_i, \Omega_j) \;=\; \sum_{n=2}^{L} \sigma_n^2 \; P_n[\, \cos\; \psi(\Omega_i, \Omega_j)\,] \;=\; C_N(\psi_{ij}) \;, \tag{18}$$

where $\psi_{ij} = \psi(\Omega_i, \Omega_j)$ is the spherical distance between directions Ω_i and Ω_j. Under these circumstances, the error covariance C_N becomes isotropic.

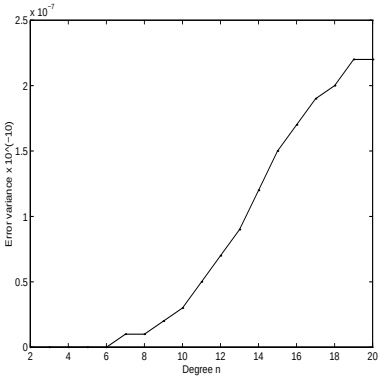

Figure 2: Error power spectrum of the GRIM4-S4 model

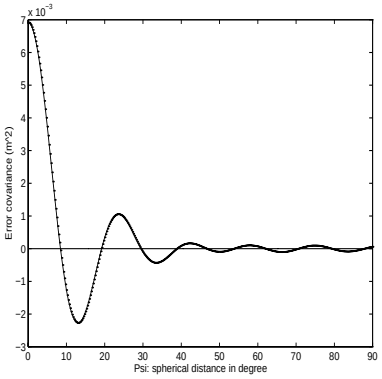

Figure 3: Error covariance function of the spheroid of degree 20 along a meridian [m^2]

3 Variance of δN and $\Delta(\delta N)$

In this section, we also omit L, simplifying δN^L to δN. The residual geoid δN obtained from the Stokes integral (Eqn. 4) is subject to errors in the gravity anomalies $\delta\Delta g^L$ in the integration domain. The error variance of the geoid is derived by the covariance law applied to the Stokes integral. Let us call this variance by $\sigma^2_{\delta N}$. It will be derived in the next section.

The difference between residual geoidal heights at points P_i and P_j is given as

$$\Delta(\delta N) \;=\; \delta N_j \;-\; \delta N_i \;, \tag{19}$$

where δN_j or δN_i are both determined from Eqn. (4). By applying the covariance law to Eqn. (19), the error variance of $\Delta(\delta N)$ is obtained as

$$\sigma^2_{\Delta(\delta N)} \;=\; \sigma^2_{\delta N}(\Omega_i) \;+\; \sigma^2_{\delta N}(\Omega_j) \;-\; 2\; C_{\delta N}(\Omega_i, \Omega_j) \;, \tag{20}$$

where $C_{\delta N}$ is the error covariance function of the residual geoid. It is related to the error correlation function $\rho_{\delta N}$ by

$$C_{\delta N}(\Omega_i, \Omega_j) \;=\; \rho_{\delta N}(\Omega_i, \Omega_j)\; \sigma_{\delta N}(\Omega_i)\; \sigma_{\delta N}(\Omega_j) \;. \tag{21}$$

3.1 Covariance of δN

Let us consider the errors in residual gravity anomalies $\delta\Delta g$ used in the Stokes integration to be statistically independent. The gravity anomalies are really not independent; they are at least correlated through errors in the reference gravity anomalies (see Eqn. 6). Dealing with this problem is out of the scope of this paper. Assuming independent anomalies, the errors of geoidal heights δN_i and δN_j, computed at two points farther than $\psi = 12°$ apart, would be statistically independent; the distance of 12° equals to twice the radius of the integration domain and for $\psi \geq 12°$, there is no overlap of the two integration domains. The statistical correlation will arise though if some data are shared by the two integrals. This will be the case for points closer than 12°, i.e., when the integration domains intersect (see Fig. 4). The area $\vartheta = C_i \cap C_j$ contains the gravity data shared by the integrations over C_i and C_j.

To formulate the covariance function $C_{\delta N}$ (Eqn. 21), we again employ an algebraic approach. Denoting by $\boldsymbol{\delta N}$ the vector of the geoidal heights computed at a mesh of m points, and $\boldsymbol{\delta\Delta g}$ the vector of gravity data required by the Stokes integral to compute $\boldsymbol{\delta N}$, we can write the following system of linear equations

$$\boldsymbol{\delta N} \;=\; \boldsymbol{S}\; \boldsymbol{\delta\Delta g} \;, \tag{22}$$

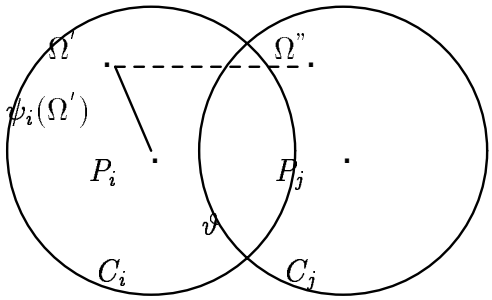

Figure 4: Intersection of the integration domains

where $\boldsymbol{S}$ is the Stokes matrix operator, with its elements

$$s_{ik} \;=\; K_i \; S^{*L}(\psi_{ik}) \; \Delta a_{ik} \;, \tag{23}$$

being the values of the Stokes kernel ($S^{*L}(\psi_{ik})$) multiplied by the area of the surface integration element (Δa_{ik}) at the gravity point P_k and by K_i (see Eqn. 4). The kernel S^{*L} runs through the spherical cap C_i of radius $\psi = 6°$, centred at point P_i. In other words, the i-th row vector of the matrix $\boldsymbol{S}$ multiplied by the vector $\boldsymbol{\delta\Delta g}$ equals to the numerical integration (summation) of the Stokes's integral (over the cap C_i), resulting in the numerical value of residual geoidal height δN_i (element of vector $\boldsymbol{\delta N}$).

Applying the covariance law to Eqn. (22) yields

$$\boldsymbol{C}_{\delta N} \;=\; \boldsymbol{S} \; \boldsymbol{C}_{\delta\Delta g} \; \boldsymbol{S}^T \;, \tag{24}$$

where $\boldsymbol{C}_{\delta\Delta g}$ is the error covariance matrix of the gravity anomalies. The element c_{ij} of the matrix $\boldsymbol{C}_{\delta N}$, is the error covariance between δN_i and δN_j. This element can be obtained from the matrix equation (above) as the quadratic form

$$c_{ij} \;=\; S_i \; \boldsymbol{C}_{\delta\Delta g} \; S_j^T \;, \tag{25}$$

where S_i and S_j are the i-th and j-th row vectors of the matrix $\boldsymbol{S}$. The operator S_i, in the spherical coordinates system, has the form

$$S_i \;=\; \left[\; \ldots \; , \; K_i \; S_i^{*L}(\Omega') \; \sin \; \psi_i(\Omega'), \; \ldots \; \right] \;, \tag{26}$$

where $\sin \; \psi_i(\Omega')$ comes from the expression of the surface integration element and $\psi_i(\Omega')$ is the spherical distance of point "Ω'" (Fig. 4) from point P_i.

The compact form of c_{ij}, denoted by $C_{\delta N}(P_i, P_j)$ in Eqn. (21) can be now written as

$$c_{ij} \;=\; C_{\delta N}(P_i, P_j) \;=\; K_i \; K_j \iint_{C_i} S_i^{*L}(\Omega') \; \sin \; \psi_i(\Omega') \; \times$$

$$\times \left[\iint_{C_j} S_j^{*L}(\Omega'') \; \sin \; \psi_j(\Omega'') \; C_{\delta\Delta g}(\Omega', \Omega'') \; d\Omega'' \right] \; d\Omega' \;, \tag{27}$$

where Ω' and $\Omega"$ are two points in the domain $\Re = C_i \cup C_j$ (Fig. 4), $S_i^{*L}(\Omega')$ is the Stokes kernel defined in the cap C_i, $S_j^{*L}(\Omega")$ is the kernel defined in the cap C_j, $\psi_j(\Omega")$ is the spherical distance of point "Ω"" from the centre P_j, K_i is the Stokes constant at P_i the centre of C_i, K_j is the constant at P_j; the centre of C_j, and $C_{\delta\Delta g}(\Omega', \Omega")$ is the covariance function (a kernel) defined for the pairs of points Ω' and $\Omega"$. The covariance function represents those "elements" of the error covariance matrix $\boldsymbol{C}_{\delta\Delta g}$ (Eqn. 24), in the compact space, that are contained in the domain $\Re$.

Assuming independent gravity anomalies ($\delta\Delta g$), then the error covariance function $C_{\delta\Delta g}(\Omega', \Omega")$ reduces to a Dirac delta function [Korn and Korn, 1968], defined as

$$C_{\delta\Delta g}(\Omega' - \Omega") \;=\; \begin{cases} 0 & for\ \Omega' \neq \Omega" \\ \sigma^2_{\delta\Delta g}(\Omega') & for\ \Omega' = \Omega" \end{cases} , \tag{28}$$

where $\sigma^2_{\delta\Delta g}(\Omega')$ is the error variance of gravity anomaly at point Ω'. Taking the delta function into account, Eqn. (27) reduces to

$$C_{\delta N}(\omega_i, \Omega_j) \;=\; K_i\, K_j \iint_{C_i} S_i^{*L}(\Omega')\, S_j^{*L}(\Omega') \;\times$$

$$\times\ \sin\,\psi_j(\Omega')\ \sin\,\psi_i(\Omega')\ \sigma^2_{\delta\Delta g}(\Omega')\ d\Omega' \ . \tag{29}$$

Further, the kernel $S_j^{*L}(\Omega')$ is different from 0 only in a portion of C_i, i.e., in the area ϑ. Hence, the integration domain (C_i) is reduced to ϑ

$$C_{\delta N}(\Omega_i, \Omega_j) \;=\; K_i\, K_j \iint_{\vartheta} S_i^{*L}(\Omega')\, S_j^{*L}(\Omega') \;\times$$

$$\times\ \sin\,\psi_j(\Omega')\ \sin\,\psi_i(\Omega')\ \sigma^2_{\delta\Delta g}(\Omega')\ d\Omega' \ . \tag{30}$$

This is the error covariance function between residual geoidal heights (δN), at points P_i and P_j, see Fig. 4.

A special case of this function is the variance $\sigma^2_{\delta N}(\Omega_i)$ at point P_i, when P_j moves towards the P_i, yielding

$$\sigma^2_{\delta N}(\Omega_i) \;\doteq\; K_i^2 \iint_{C_i} \left[\ S_i^{*L}(\Omega')\ \sin\,\psi_i(\Omega')\ \right]^2\ \sigma^2_{\delta\Delta g}(\Omega')\ d\Omega' \ . \tag{31}$$

As P_j moves to P_i, the integration domain ϑ increases to C_i. Writing error variances at points P_i and P_j, and assuming uniform accuracy $\sigma^2_{\delta N}(\Omega')$ for the gravity anomalies, and taking $K_i \doteq K_j$, the correlation function $\rho_{\delta N}$ is obtained from Eqn. (21). Substituting for the error covariance and variances from Eqns. (30) and (31) we get

$$\rho_{\delta N}(\Omega_i, \Omega_j) \;= \tag{32}$$

$$= \frac{\iint_{\vartheta} S_i^{*L}(\Omega') \; S_j^{*L}(\Omega') \; \sin \; \psi_j(\Omega') \; \sin \; \psi_i(\Omega') \; d\Omega'}{\sqrt{\iint_{C_i} [S_i^{*L}(\Omega') \; \sin \; \psi_i(\Omega')]^2 \; d\Omega'} \; \sqrt{\iint_{C_j} \left[S_j^{*L}(\Omega') \; \sin \; \psi_j(\Omega')\right]^2 \; d\Omega'}} \; ,$$

and realizing that $C_i = C_j = C_0$, we finally get

$$\rho_{\delta N}(\Omega_i, \Omega_j) \; = \; \frac{\iint_{\vartheta} \; S_i^{*L}(\Omega') \; S_j^{*L}(\Omega') \; \sin \; \psi_j(\Omega') \; \sin \; \psi_i(\Omega') \; d\Omega'}{\iint_{C_0} [\; S_0^{*L}(\Omega') \; \sin \; \psi_0(\Omega') \;]^2 \; d\Omega'} \; , \tag{33}$$

where $S_0^{*L}(\Omega')$ is the Stokes kernel, defined in the spherical cap C_0. Clearly, as $P_j \rightarrow P_i$, $\rho_{\delta N}(\Omega_i, \Omega_j) \rightarrow 1$, as it should.

3.2 Numerical Evaluation of $\rho_{\delta N}$

The correlation function can now be numerically evaluated. The modified spheroidal Stokes kernel can be approximated within the 6° spherical cap by the function

$$S'(\psi) \doteq -32.43544 + \frac{1.99727}{\psi} - 3.44927 \; \ln\left(\frac{\psi}{2}\right) - 173.24417 \; \psi^2 \; \ln\left(\frac{\psi}{2}\right) \; , \tag{34}$$

to the accuracy of better than 10^{-3} [Vaníček and Kleusberg, 1987]. This accuracy was shown to be good enough for evaluating the geoid with an error less than 10 cm [ibid] and it is certainly good enough for evaluating the correlation in practice, where an error of 1% should be considered small enough. The correlation function, Eqn. (33), is the ratio of two surface integrals. In the denominator is the integral of the squared Stokes's kernel over the whole spherical cap of radius $\psi_0 = 6°$. The integrand is singular at the centre of the cap, but the singularity is removed in the spherical coordinates system. The integral is finite and equals approximately to 0.9558. We note that this number seems to be acceptably close to 1.

The integral in the numerator is taken over the intersection area ϑ, and involves the product of two kernels, referred to points P_i and P_j, Fig. 5. The integral is written in a more explicit form as

$$\iint_{\vartheta} \; S^{*L}(\psi_i(\Omega_i, \Omega')) \; S^{*L}(\psi_j(\Omega_j, \Omega')) \; \sin \; \psi_j(\Omega') \; \sin \; \psi_i(\Omega') \; d\Omega' \; , \tag{35}$$

where Ω_i and Ω_j define the points P_i and P_j, ψ_i and ψ_j are the spherical distances, and Ω' defines the dummy point P'. At a first look, the integral seems to be a function of Ω_i and Ω_j, but writing the integral in the polar coordinate system at the pole P_i with polar coordinates of ψ_i and α (azimuth) as

$$I(\psi) \; = \; \iint_{\vartheta} S^{*L}(\psi_i) \; S^{*L}(\psi_j(\psi, \psi_i, \alpha)) \; \sin \; \psi_j(\psi, \psi_i, \alpha) \; \sin \; \psi_i \; d\psi_i \; d\alpha \; , \tag{36}$$

where ψ_j (see the triangle $P_iP'P_j$) is a function of ψ_i, ψ, and the azimuth α, shows that the integral is really a function of ψ – the spherical distance between points P_i and P_j.

For the numerical evaluation of the correlation function, a planar approximation is employed: the spherical caps C_i and C_j are regarded as plane circles. Fig. 5 illustrates the case of $\psi < \psi_0$. In this case, the area of the integration is divided into four quadrants: OAD, OAB, OBC, and OCD. Because the Stokes kernel is homogeneous and isotropic, the integral over the area ϑ equals to four times the integral over, for instance, the area OAB,

$$I(\psi) \;=\; 4 \iint_{(OAB)} S^{*L}(\psi_i)\; S^{*L}(\psi_j)\; \sin\; \psi_j\; \sin\; \psi_i\; d\psi_i\; d\alpha\;. \tag{37}$$

In the area (OAB), the kernel $S^{*L}(\psi_i)$ remains a regular function, while the kernel $S^{*L}(\psi_j)$ is singular at point P_j. The integration is carried out in the polar coordinate system with origin at P_i, and the singularity is treated separately. In the case $\psi > \psi_0$, see, i.e., Fig. 4, the integration can be again divided into 4 segments in the same coordinate system, provided that there would be no singularity of the Stokes kernels in this case. The correlation function obtained is shown in Fig. 6; it decreases monotonically, from unity at the 0° spherical distance to zero at a spherical distance of 12°.

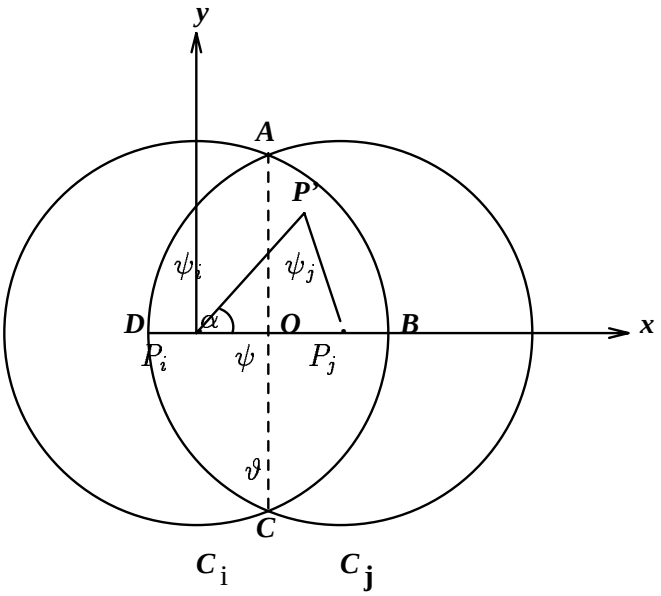

Figure 5: Integration over the area ϑ, for $\psi < \psi_0$

The integration was performed numerically for $\psi \in < 0, 12° >$ at a step of 0.01 degree of arc in both variables. For practical applications, the correlation function can be

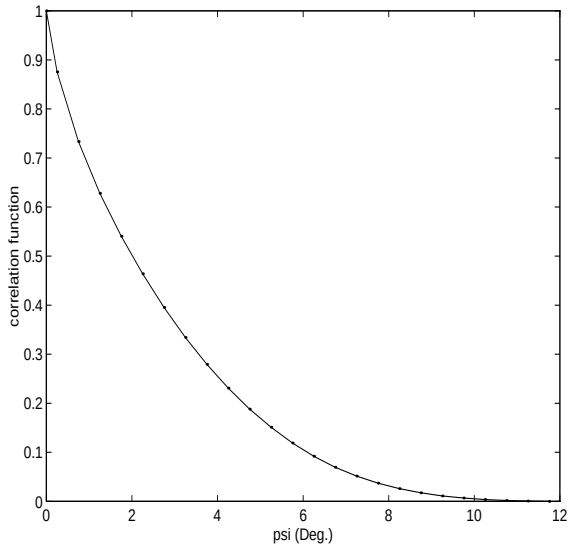

Figure 6: Correlation function of the residual geoid

approximated by the following function

$$\rho_{\delta N}(\psi) \;=\; 1 \;+\; a \;\ln\,(1+\psi) \;+\; b\;\psi^3 \;, \tag{38}$$

to the accuracy of 0.01 (root mean squares error of fit), where

$$\begin{aligned} a &= -\,0.46824364 \;, \\ b &= +\,0.00012060 \;, \end{aligned}$$

for ψ expressed in degrees of arc.

3.3 Relative Accuracy of the Geoid

The accuracy of the geoid, σ_N^2, is obtained from Eqn. (7) by applying the covariance law

$$\sigma_N^2 \;=\; \sigma_{N_L}^2 \;+\; \sigma_{\delta N^L}^2 \;, \tag{39}$$

where on the right hand side are the variances of the spheroid and the residual geoid, considered here independent. In fact, these variances are statistically dependent (correlated), due to the use of Δg_L in derivation of $\delta\Delta g^L$ (see Eqn. 6). The correlations call for a separate investigation.

For the investigation of relative accuracy, Eqn. (7) is re-written for the differences of quantities involved, as

$$\Delta N \;=\; \Delta N_L \;+\; \Delta(\delta N^L) \;. \tag{40}$$

For the reason just discussed, the relative quantities (above) are also correlated. In the case of a higher degree spheroid (360×360) being used as a reference [She et al., 1993], there are even correlations between Δg_L and the "observed" Δg, too. Assuming independence and applying the variance law to Eqn. (40), we obtain the error variance of the geoid difference as the sum

$$\sigma^2_{\Delta N} \;=\; \sigma^2_{\Delta N_L} \;+\; \sigma^2_{\Delta(\delta N^L)} \;, \tag{41}$$

of the variances of the two components.

After the correlation functions for the spheroid and the high-frequency geoid are derived (Eqns. 12 and 20), they are added together to give the variance of the total geoidal height differences. We obtain

$$\begin{aligned} \sigma^2_{\Delta N} \;=\; & \sigma^2_N(\Omega_i) \;+\; \sigma^2_N(\Omega_j) \;-\; 2\;\rho_N(\Omega_i,\Omega_j)\;\sigma_N(\Omega_i)\;\sigma_N(\Omega_j) \;+ \\ & + \;\sigma^2_{\delta N}(\Omega_i) \;+\; \sigma^2_{\delta N}(\Omega_j) \;-\; 2\;\rho_{\delta N}(\Omega_i,\Omega_j)\;\sigma_{\delta N}(\Omega_i)\;\sigma_{\delta N}(\Omega_j)\;. \end{aligned} \tag{42}$$

4 Numerical Results

To show the error correlation in geoid computation, seven points on the meridian of 240° east were selected. The first point is located at the latitude of 45° north and the last at the latitude of 70° north. The spacing between adjacent points is 1°, 2°, 4°, 6°, 10°, 25°, respectively, see Tab. (1). Table (2) refers to the spheroid of degree 20, using the GRIM4-S4 geopotential model. The covariance matrix was evaluated from Eqn. (15). Standard deviations (SD), i.e., the square root of the diagonal elements of the covariance matrix, are also shown in this table. Table (3) displays the error correlation coefficients for the residual geoid, computed from Eqn. (37), while Tab. (4) shows the corresponding error covariances, both for the UNB '86 geoid model [Vaníček et al., 1986]. Table (5) presents the complete geoid (the sum of the spheroid and the residual geoid) at the selected seven points, and the corresponding covariance matrix (the sum of the matrices shown in Tabs. (2) and (4). Finally, Tab. (6) shows the geoidal height differences and their standard deviations, computed using Eqn. (41), all referred to the southernmost point.

5 Conclusions

The error covariance function of spheroid (Fig. 3), show positive correlation between spheroidal heights of two points at distances less than 900 km. This indicates a better relative accuracy than the absolute accuracy of the spheroid, i.e., the errors in the satellite-derived field are somewhat canceled out in spheroidal height differences. In the residual

geoid, the correlation function decreases to zero at 12° spherical distance between two points. The correlation is a function of the area covered by the gravity data, shared by the Stokes integrals at the two points. The correlation is positive (Fig. 6), indicating again a better relative accuracy of the residual geoidal heights. In the derivation of the correlation function, the observations (surface gravity anomalies) have been assumed statistically independent and of uniform accuracy. In the real situation, however, the gravity anomalies are statistically correlated and are usually of different accuracies. The impact of this on the residual geoid correlation has not been investigated here.

Acknowledgement

We are truly grateful to Pavel Novák for his able and unselfish assistance with the preparation of the LaTeX version of this paper.

No	Latitude	Longitude
1	45°	240°
2	46°	240°
3	48°	240°
4	52°	240°
5	58°	240°
6	68°	240°
7	70°	240°

Table 1: Positions of seven test points

No	S_{20} [m]	SD [m]	Cov						
1	-18.541	0.081	0.007						
2	-17.650	0.082	0.006	0.007					
3	-16.345	0.084	0.005	0.006	0.007				
4	-15.074	0.089	-0.002	0.000	0.004	0.008			
5	-14.328	0.102	-0.006	-0.006	-0.005	0.001	0.010		
6	-14.602	0.119	0.002	0.002	0.001	-0.003	-0.004	0.014	
7	-14.310	0.121	0.002	0.002	0.002	-0.001	-0.005	0.013	0.015

Table 2: Spheroid S_{20} and its covariance matrix

No	Cor						
1	1.0000						
2	0.6756	1.0000					
3	0.3541	0.4865	1.0000				
4	0.0677	0.1149	0.2541	1.0000			
5	0.0000	0.0000	0.0020	0.1149	1.000		
6	0.0000	0.0000	0.0000	0.0000	0.002	1.0000	
7	0.0000	0.0000	0.0000	0.0000	0.000	0.4865	1.0000

Table 3: Matrix of correlation coefficients

No	δN_{20} [m]	SD [m]							
1	-0.76	0.04	0.0016						
2	-3.41	0.04	0.0011	0.0016					
3	-3.53	0.06	0.0008	0.0012	0.0036				
4	-0.71	0.19	0.0005	0.0009	0.0029	0.0361			
5	0.62	0.35	0.0000	0.0000	0.0000	0.0076	0.1225		
6	2.56	0.09	0.0000	0.0000	0.0000	0.0000	0.0000	0.0081	
7	-0.35	0.08	0.0000	0.0000	0.0000	0.0000	0.0000	0.0035	0.0064

Table 4: UNB'86 "residual geoid" (δN_{20}) and its covariance matrix

No	N [m]	SD [m]							
1	-19.301	0.09	0.0086						
2	-21.060	0.09	0.0071	0.0086					
3	-19.875	0.10	0.0058	0.0072	0.0106				
4	-15.784	0.21	-0.0015	0.0009	0.0069	0.0441			
5	-13.708	0.36	-0.0060	-0.0060	-0.0050	0.0086	0.1325		
6	-12.042	0.15	0.0020	0.0020	0.0010	-0.0030	-0.0040	0.0221	
7	-14.660	0.15	0.0020	0.0020	0.0020	-0.0010	-0.0050	0.0165	0.0214

Table 5: Total geoid (spheroid + residual geoid) and its covariance matrix

No	Distance [m]	ΔN [m]	SD [m]	Error per unit distance [10^{-6}]
1		0.000	0.000	
2	0110	-1.759	0.055	0.50
3	0330	-0.574	0.087	0.26
4	0770	3.517	0.236	0.31
5	1430	5.593	0.391	0.27
6	2530	7.259	0.163	0.06
7	2750	4.641	0.161	0.06

Table 6: Geoidal height differences and their standard deviations

References

Gruber, T. and M. Anzenhofer (1993). The GFZ360 Gravity Field Model, the European Geoid Determination. Proceedings of session G3, European Geophysical Society XVIII General Assembly, Wiesbaden, May 3-7, 1993 (published by the Geodetic Division of KMS, Kopenhagen).

Heiskanen, W. A. and H. Moritz (1981). *Physical Geodesy.* Reprinted in the Institute of Physical Geodesy, Technical University Graz, Austria.

Korn, G. A. and T. M. Korn (1968). *Mathematical Handbook for Scientists and Engineers.* McGraw-Hill book company, New York.

Schwintzer, P., Ch. Reigber, A. Bode, Z. Kange, S. Y. Zhu, F. H. Massmann, J. C. Raimondo, R. Biancale, G. Balmino, J. M. Lemoine, B. Moynot, J. C. Marty, F. Barlier, and Y. Boudon (1995). Long-wavelength Global Gravity Field Models GRIM4-S4, GRIM4-C4. GeoForschungsZentrum (GFZ, Div. I), Potsdam, and Groupe de Recherche de Géodésie Spatiale (GRGS), Toulouse, Grasse.

She, B. B., M. G. Sideris, and K. P. Schwartz (1993). A PC-based Unified Geoid for Canada. Final report for DSS contract No. 23244-0-4451/01-ET. The University of Calgary, Department of Geomatics Engineering.

Sideris, M.G. and K.P. Schwartz (1987). Improvements of Medium and Short Wavelength Features of Geopotential Solutions by Local Data. *Boll. Geod. Sci. Affini*, XLVI, 3, 207-221.

Vaníček, P. and E. J. Krakiwsky (1986). *Geodesy: The Concepts.* 2nd corrected ed., North Holland, Amsterdam.

Vaníček, P. and A. Kleusberg (1987). The Canadian Geoid – Stokesian Approach. *Manuscripta Geodaetica* 12, 86-98.

Vaníček, P., A. Kleusberg, R. G. Chang, H. Fashir, N. Christou, M. Hofman, T. Kling, and T. Arsenault (1986). Technical Report No. 29, Dept. of Surveying Engineering, University of New Brunswick, Fredericton.

Vaníček, P. and L. E. Sjöberg (1991). Reformulation of Stokes's Theory for Higher than Second-Degree Reference Field and a Modification of Integration Kernels. *JGR* 96(B4), 6529-6539.

Vaníček, P. and Z. Martinec (1994). The Stokes-Helmert Scheme for the Evaluation of a Precise Geoid. *Manuscripta Geodaetica*, 19, 119-128.